British Journal of Applied Science & Technology
4(31): 4356-4379, 2014
ISSN: 2231-0843

SCIENCEDOMAIN *international*
www.sciencedomain.org

Resistance to Thaumasite form of Sulphate Attack of Blended Cement Mortars

Hanifi Binici[1*], Selim Kapur[2], Tamer Rızaoğlu[3] and Mehmet Kara[1]

[1]Department of Civil Engineering, Kahramanmaraş Sütçü Imam University, Kahramanmaraş, Turkey.
[2]Department of Soil Science, Çukurova University, Adana, Turkey.
[3]Department of Geological Engineering, Kahramanmaraş Sütçü Imam University, Kahramanmaraş, Turkey.

Authors' contributions

This work was carried out in collaboration between all authors. All authors read and approved the final manuscript.

Article Information

DOI: 10.9734/BJAST/2014/11948
Editor(s):
(1) Saumitra Mukherjee, School of Environmental Sciences, Jawaharlal Nehru University (JNU), India.
(2) Abida Farooqi, Department of Environmental Sciences, Quiad-i-Azam University, Pakistan.
Reviewers:
(1) Anonymous, NED University of Engineering and Technology, Pakistan.
(2) Anonymous, Council for Scientific and Industrial Research—Building and Road Research Institute, Ghana.
Peer review History: http://www.sciencedomain.org/review-history.php?iid=635&id=5&aid=5914

Original Research Article

Received 11th June 2014
Accepted 30th July 2014
Published 26th August 2014

ABSTRACT

This study concerns the resistance against thaumasite form of sulphate attack on Portland cement reference with high volume ground granulated blast-furnace slag, fly ash and ground basaltic pumice exposed to tap water (5% magnesium sulphate) for ten years. The separate and intergrinding methods, two fineness (250m^2/kg and 500 m^2/kg) and 30% proportions of each of the different additives were employed in equal amounts by weight. The development of the microstructure and the secondary minerals in the plain and blended cements were studied via polarising microscopy on thin sections and on undisturbed lumps of specimens by scanning electron microscope (SEM-EDAX) analysis. A series of mechanical tests of cement mortars were undertaken on all specimens. The

**Corresponding author: E-mail: hbinici@ksu.edu.tr;*

development of the microstructural features and the formation of the secondary minerals in pores were coherent to the increase in sulphate resistance. The presence of thaumasite together with ettringite in some specimens reflects the incomplete transformation phase of hydration. However, despite the numerous studies conducted on the relation of hydration and hydrolysis with reference to cement hardening, the hydration-bound hardening phenomenon coupled with thaumasite morphology and matrix and/or pore space orientations are recommended for further investigation. The use of the pozzolans/ground granulated blast furnace slag and basaltic pumice improved the sulphate resistance of the cement mortars, where specimen E yielded the highest sulphate resistance-highest TSA resistance.

Keywords: Microstructure; magnesium sulphate resistance; thaumasite/ettringite.

1. INTRODUCTION

Recently, there has been a growing demand towards the use of supplementary cementitious materials, be it natural, waste, or by-products, the production of composite cements because of ecological, economical, and diversified product quality reasons. Slag, a by-product of the transformation of iron ore into pig-iron in a blast furnace, is one of these materials in use of cement manufacturing dating to as far back as 1880 [1-3]. Since then, its use has expanded due to its various advantages over other cementitious materials. As a primary advantage, slag has a relatively constant chemical composition compared to fly ash, silica fume and natural pozzolan [4-8].

Durability of concrete in underground structures depends on chemical properties of soil and groundwater. A sulphate or an acid environment caused by industrial wastes, or chemical residues in reclaimed ground, is one of the most severe conditions for durability of concrete. Unfortunately, underground or underwater concrete structures can sometimes be exposed to sulphates and acids, since ater-soluble sulphate widely exists in soil, groundwater, streams, and seawater [9-12]. It has been recognised for a long time that sulphte induces damage to concrete. Some researchers have reported that the use of low water/cement ratio and the use of admixtures, such as air entraining agents to protect the chemical attack of a rich mixture, additive, or Ground Blast furnace slag (GBFS), would be the most effective treatment in reducing sulphate-inducing damage [13,14]. Deterioration of concrete by sulphate attack is commonly observed in structures exposed to soils or groundwater containing a high concentration of sulphate ions. To mitigate this attack, concrete codes recommend a concrete mixture with low water/cement ratio and sulphate resistant pozzolanic cement [15].

The European Cement Standards and The Turkish standards [16,17] allow the use of many different mineral admixtures in the production of CEM II, III, IV and V. It is necessary to note that Portland composite and composite cements contain at least two different mineral admixtures besides the Portland cement clinker. The total amount of these mineral admixtures is allowed up to 50% [18]. The durability of mortars can be greatly affected by environmental conditions, one of the most destructive effects coming from sulphates (soil, groundwater and seawater).

Wearing effects of chemical materials to concrete can be in various ways, acids induce dissolving salts in water to react with calcium hydroxide. Salts in concrete increase permeability and reduce resistance against harmful effects, whereas sulphates cause

distensions and cracking in concrete**.** This damage depends on the cations taking part in building gypsum and ettrengite or the decomposition of CSH gels. The majority of these wearing reactions depend on the increase of the C_3A content in concrete with high negative effects [19]. An example for the negatıve effects of C3A.Commonly, 15% silica ash is added together with pumice in order to reduce the amount of C_3A. However, by creating an initial resistance against damage, silica ash and pumice reduce permeability as an operative effect along with highly active calcium hydroxide [20].

The sulphate wearing, concerning increases in volume and cracks of concrete, is reduced by the the use of low ratios of tricalcium aluminate cements or suitable amounts of pumice as additives. Tricalcium aluminate indirectly decreases by the addition of pumice, and fills the pores in concrete as a connective component by joining with lime [21].

Calcium, sodium, magnesium and ammonium sulphate cause significant amounts of expansion in concrete consequently decreasing the strength. Calcium sulphate reacts with calcium aluminate to form ettrengite, and in turn, causes expansion in concrete, whereas, ammonium sulphate is responsible for the highest corrosion in concrete bodies [22]. Moreover, sodium sulphate reaction has been reported to cause expansion and cracking in concrete by initial ettringite and gypsum formation followed by the ultimate development of thaumasite [23].

A long-known and major sulphate attack in concretes and mortars is caused by the formation of thaumasite, which forms under low temperatures as well as room temperatures (25 degrees C) and at wet, alkaline conditions extensively experienced at buried concrete structures [24]. For the development of the thaumasite form of sulphate attack (TSA) in concrete the presence of a carbonate source is indispensable for an alkaline environment [25]. This can be supplied to the concrete structure from the ingredients of the concrete or from outside sources like groundwater, surface water or seawater which is also the source of sulphate [26,27]. Some recent studies revealed the absence of TSA at 5 and 25 degrees Celcius in blends containing limestone additives treated with sulphate solutions [28,29]. TSA is also reported to occur in Portland cement-based materials at low temperatures (below15ºC) at the presence of sulfates, carbonates, andmoisture. Consequently, the dissolution–precipitation mechanism in concrete concerns most processes and phenomena including the temperature of the reactive environment occurring during the TSA process [30].

We have opted to reveal in this paper the durability/resistance of the separate and intergrinded blended cements with the incorporation of some additives within a 10-years time span under the effect of a $MgSO_4$ solution at room temperature with special attention on TSA. The fineness of the control cement (clinker + gypsum) was maintained at constant values of approximately 250 and 500 m^2/kg. Similar Blaine values were determined for the blended cement (clinker + slag + fly ash + pumice + gypsum) and the control specimen.

2. MATERIALS AND METHODS

2.1 Materials

Ground basaltic pumice (GBP), obtained from the widespread Delihalil cinder cone system in Osmaniye, Turkey, is one of the main additives used in this study. It contains glass shards, mineral phases and some volcanic materials [31]. The clinker, ground granulated blast-furnace slag (GGBFS) and the fly ash (FA)-were obtained from the Adana Cement Plant, the Iskenderun cement grinding plant and the Afsin-Elbistan energy plant respectively.

2.1.1 Physical and chemical properties of the additives

Slag and Pumice were the high silica, alumina, magnesium and iron (in pumice only) containing additives of the mortars studied, and the fly ash was the material rich in calcium, and sulphur in particular (Table 1). The physical properties of the materials used varied slightly in specific gravity and for the two fineness ranges. The specific surface areas were the same in each mixture (Table 2). The uniform blended cement mixture was obtained by two different methods. The first was by grinding of the mixture separately for ten minutes. And for the second, blended cement mixture ratios were determined and ground. The B and C group samples were ground separately, whereas the D and E group samples were ground together.

Table 1. Total elemental contents of the additive materials

Contents	SiO_2	Al_2O_3	Fe_2O_3	CaO	MgO	SO_3	L.I
Slag	39.65	12.77	1.67	32.91	7.40	1.44	0.01
Flyash	44.09	22.07	4.40	20,95	1.65	2.56	2.24
Pumice	43.89	14.11	12.10	9.27	8.94	-	0.48
Clinker	20.29	5. 57	3. 85	64.75	1.96	0.89	

Table 2. Physical properties of the additives

Contents	Specific gravity (kg/cm^3)	Specific surface area (m^2/kg)	200 μm fraction (%)	90 μm fraction (%)
Slag	2.89	250 and 500	0.09	0.3
Flyash	2.85	250 and 500	0.08	0.2
Pumice	2.97	250 and 500	0.06	0.2
Clinker	3.19	250 and 500	0.09	0.3

2.2 Methods

2.2.1 Physical and chemical methods

The specific gravity and the specific surface area were determined by a method developed in accordance with ASTM-C204. The ball mill grindability tests were conducted in a standard Ball mill for the 90 micron test sieve. The basaltic pumice, the slag and the clinker were reduced down to the same fineness by crushing in the roll crusher. The 3.36 mm specimens were used as feed materials for the tests. The more grindable gypsum tends to be concentrated in the finer particle size fractions of the product during the grinding process. Particle size distribution was measured by laser diffraction. Blaine fineness values were determined according to the ASTM-C204 [4].

Total elemental contents of additives and blends (Table 3) were determined by the wet combustion method. The size fractions of 90 and 200 microns were separated through Standard ASTM. The chemical analyses are put after the physical for consistency with the subtitle which mentions the physical properties first and chemical second.

2.2.2 Blended cements preparation, mortar formation and curing

The blended cements were prepared using a clinker, 5% gypsum by weight, GGBS, FA and GBP. Equal amounts of additives (30%, by weight) were incorporated into these blends. Cement paste and mortars were prepared using plain Portland cement (A), GGBS, FA and GBP by two types of grinding processes (intergrinding and separate grinding) at two Blaine values (250 m^2/kg and 500 m^2/kg) (Table 3). The first grinding method was conducted by grinding the mixture separately for ten minutes at a non-marble grinder, and the second included the grinding of triple mixture ratios. The B and C group samples were ground separately, whereas the D and E group samples were ground together.

The mortar specimens of the plain Portland cement (A1, A2) and the blended cements (B, C, D and E) were prepared according to the Rilem-Cembureau method at laboratory conditions (20±2ºC and 50±5% relative humidity). Following the 24-hour demolding, the specimens were kept in water until they were tested. Six specimens with dimensions 40 mm×40 mm×40 mm, obtained from the specimens used in the flexural strength tests, were tested under the same laboratory conditions as those applied in the flexural strength test. Thec compressive strength tests were carried out using a 20000 kN capacity automatic compression machine according to EN 196-1 [4].

Table 3. The composition of the studied cements

Cement	Composition (% percentages by weight)					Blaine (m^2/kg)
	Clinker	GBFS	FA	GBP	Gypsum	
A_1	95	0	0	0	5	250
A_2	95	0	0	0	5	500
B (separate grinding)	65	10	10	10	5	250
C (separate grinding)	65	10	10	10	5	500
D (intergrinding)	65	10	10	10	5	250
E (intergrinding)	65	10	10	10	5	500

2.2.3 Experimental setup

Sulphate durability, compressive strength and microstructure studies (by polarising and scanning electron microscopy) were conducted on standard 40 x 40 x 160 mm prismatic mortar specimens treated in a $MgSO_4$ solution for a 10-year period at stable pH levels. The solution was replaced at regular periods. Compressive strength of the mortar specimens was determined after the 10-year treatment period. Although the sulphate contents of natural or polluted waters may vary in amounts, the sulphate of most stream and luke water systems seldomly exceeds the 100 mg/l limit. Numerous studies have mentioned the increase in sulphate resistance of cement, and rapid experimental methods were developed to determine the behaviour of additives

Mixtures and control specimens of mortars were tested according to ASTM C 1012 standards for compressive strength. Here mixtures were tested via twelve parallel specimens based on the TS EN 24 Standards after treatment for 24 hours in laboratory conditions. After 24 hours, specimens were kept in lime-rich tap water for 28 days; the durability of mixtures was determined on these specimens, and the remaining specimens were kept in tap water and magnesium sulphate solutions. The pH of the Mg solution was periodically checked by a pH-meter to attain consistency in alkalinity (for the first 6 months varied from pH 8 to 11 after that date it was kept consistent from pH 11.5 to 12). Samples

were then stored in boxes and the solution was stirred from time to time to avoid sulphate accumulation on the surface. After the 10-year treatment period, both durability and microstructure of the specimens were determined. The utilization of the pozzolans in mortars can cause cracking and weakening due to expansion by alkali–silica reaction (ASR). In this study, ASR expansion and properties of strength were analysed in terms of pozzolan used, in anticipation of reducing ASR expansion.

2.2.4 Micromorphology (microstructure/fabric) and mineralogy (x-ray diffraction and x-ray flourescence)

Thin sections were prepared according to FitzPatrick [32] from epoxy resin impregnated blocks. Undisturbed lumps of mortar were studied by sub-microscopy (scanning electron microscopy-SEM) on selected cement prisms, which were exposed to sulphate degradation for 10 years and cut into cubes of approximately 10 mm^2, one side of which was polished flat. The lumps taken from the specimens were placed in vacuum desiccators for a minimum period of 10 minutes. Sample surfaces were coated with gold using a BIO-RAD Polar Division SEM coating system and the microstructure of the specimens was studied by a JEOL JEM–8,40 SEM with a TRACTOR–TN 5502 model Energy Dispersion Spectrometer (EDS) used for point and area chemical analyses. A Bruker D8 General Area Detector for diffractometry and copper target with a scanning angle from 38 to 90 2-theta was used for XRD analysis conducted on the same, but ground specimens used for SEM. X-ray diffraction was conducted on the ground powder samples of all specimens from 5 to 65 2-theta in order to determine the secondary minerals formed in the blends. The powdered specimen E was rescanned from 5 to 65 2-theta and its elemental contents were determined by XRF primarily to better distinguish the proximate thaumasite and ettringite peaks obtained by XRD analysis. This was also an attempt to explain the nature of the vitrified-like surfaces on the edges of specimen E determined by the SEM.

3. RESULTS AND DISCUSSION

3.1 Compressive Strength of Mortars Immersed in Magnesium Sulphate

The separately produced blended cement specimens (B and C) were determined to have lower resistance to sulphate than the interground, where specimen C was higher than specimen B in terms of compressive strength (Table 4). The control specimens (A1 and A2) were found to completely crumble at the end of the 10-year period (Fig. 1). The intergrinding process was responsible for the10-year high sulphate resistance due to different grinding periods and additives [6].

Table 4. Compressive strength of mortars (MPa)

Specimens	28 days	10 years	
		Tap water	%5 $MgSO_4$
A_1	52.1	66.1	Crumbled-
A_2	58.4	69.4	Crumbled-
B	36.2	56.9	22.1
C	52.3	67.1	27.4
D	37.5	58.1	22.6
E	54.2	69.6	29.4

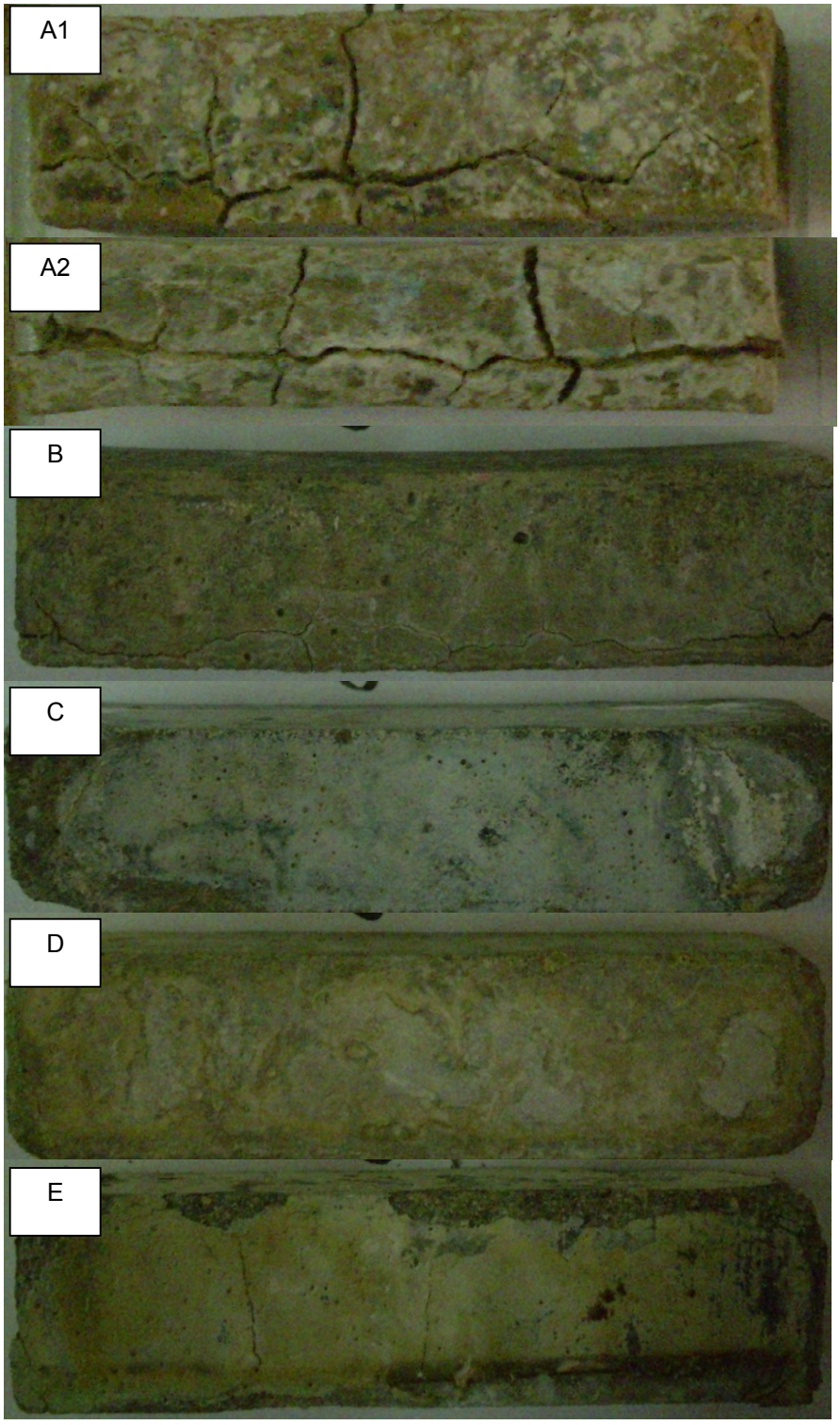

Fig. 1. Theblendedcementmortarsafter ten years

3.2 Expansion of the Specimens

The expansion–time history curve that was made by measurements complying with ASTM C 1260 in terms of the specimens of 250 Blaine and of 500 Blaine is shown in Figs. 2 and 3. Fig. 2 shows the variation of expansion of hardened mortars with two Blaine values. The expansion of the mortars made with blended cements with separately ground finer specimens was lower than that of the control specimens (A1 and A2) at all tested ages. The control cement mortar expanded by more than 4,5% in 10 years. The expansion of the hardened blended cement mortars was affected not only by the finenesses of the cements, but in some cases, also by the grinding method. Specimen group E had the lowest expansion in 10 years and the expansions of samples A2, B and D were 3.4 %, 1,1 and 0.8%, respectively (Fig. 2). The Blaine specific surface area is the most significant property causing interground specimens to have lower expansion than their separately ground counterparts.

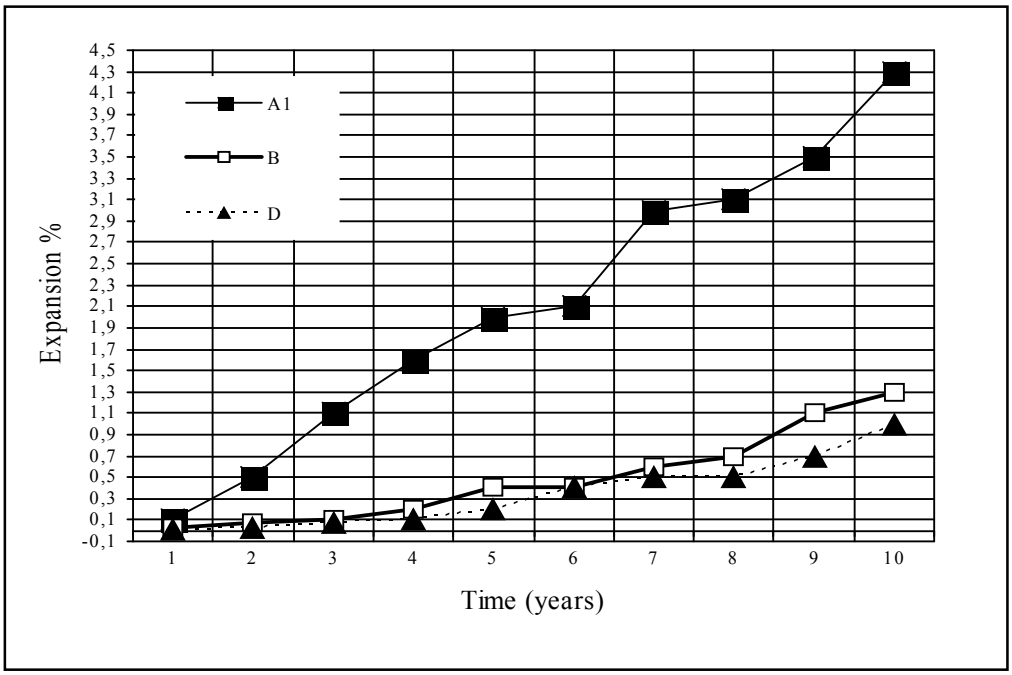

Fig. 2. Expansion time histories for mortar bars (250 Blaine)

3.3 Micromorphology (Microstructure/Fabric) and Mineralogy

3.3.1 Submicroscopy

The crumbling of the A1 and A2 specimens after the 10-year period was most likely due to the formation of the bladed/tabular minerals along cracks and in micro-pores (Fig. 4 and 5). The presence of high amounts of silica, most likely liberated from the solution of quartz grains under high pH conditions, documents the formation of thaumasite, as bladed and wedge clustered radially oriented fibrous crystals, in specimen A1. However, the low amounts of aluminum with calcium may point out to the formation of ettringite together with the well-defined dominant fibrous thaumasite in specimen A2 (Figs. 4 and 5).

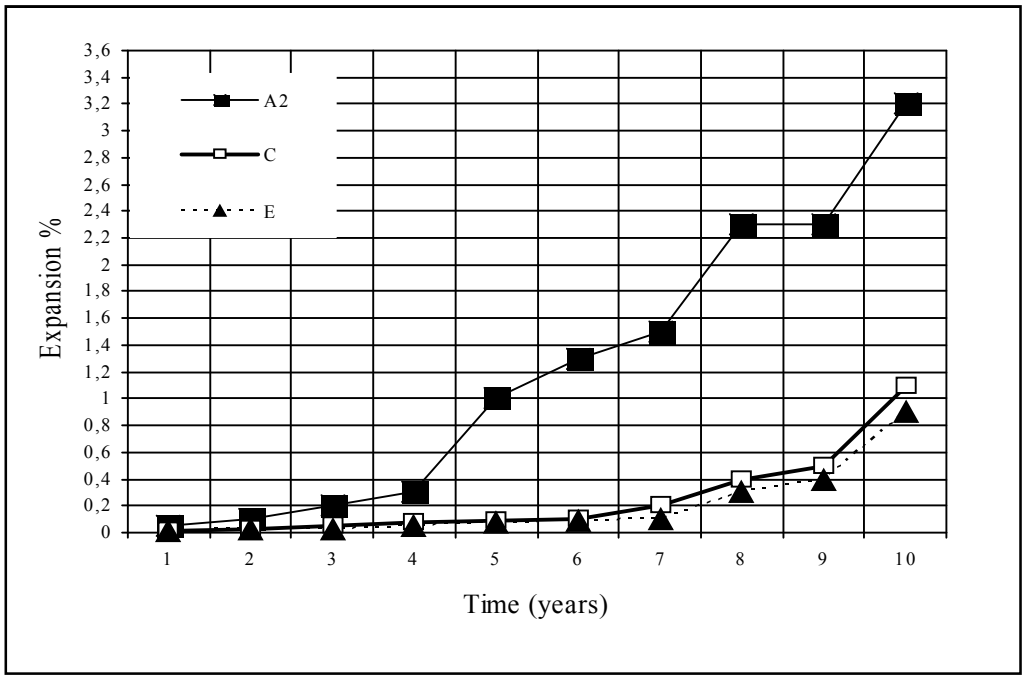

Fig. 3. Expansion time histories for mortar bars (500 Blaine)

The highest durability determined in the 10-year tap water treated A2 specimen seems to contradict the crumbling of the $MgSO_4$ treated A2 specimen. Despite the higher contents of calcium and carbonate ions in the tap water (208 mg/lt), this phenomenon may be attributed to the more active ionic effects of magnesium and sulphate added to the solution. The sulphate in this context maintains the electroneutrality, due to the counterdiffused OH ions, consequently increasing the pH (33).Calcium, in turn, is most likely widely incorporated into the mineral structure, primarily for calcite formation, during the pH-controlled high alkaline curing process, consequently remaining inert throughout the 10-year period. The well crystallised and oriented rhombohedric calcite crystals of uniform shape with rare rounded vaterite (fine popcorn calcite) on quartz and cracked matrix surfaces in specimen B and D respectively, most likely indicate the long- period of curing under constant pH conditions (Figs. 6 and 9). The fine popcorn calcite along with the unstable vaterite may also be the cause for the low durability of the mixed specimens. The increased durability of specimen C to B and E to D, after treatment, is primarily due to the increased fineness of specimens C and E and the relevant fabric development (Table 5). As reported previous study of Binici [6] Blaine specific surface area is the most significant property causing interground specimens to have longer dormant periods (the period in which sulfates have no important effect) than their separately ground counterparts. Moreover, the higher durability in specimen C may be attributed to the re-oriented fabric due to the presence of the in-situ formed and closely packed/interlocked coarser aggregates of calcite with gypsum, CSH structures and bundles of thaumasite and/or ettringite fibers (Figs. 7 and 8). However, the increased durability of specimen E may be due to the frequently distributed aggregates of calcite, gypsum and CSH structures which also align on micro-topographic edges of the smooth/vitrified-like matrix surfaces as thick domains (Fig. 10).

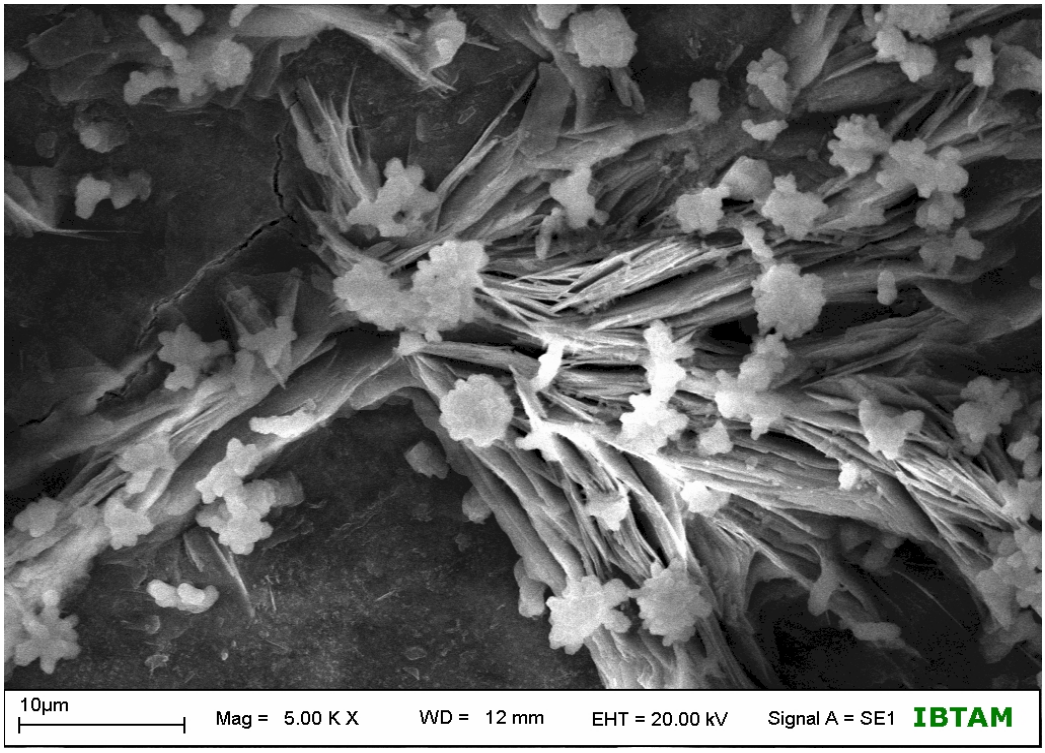

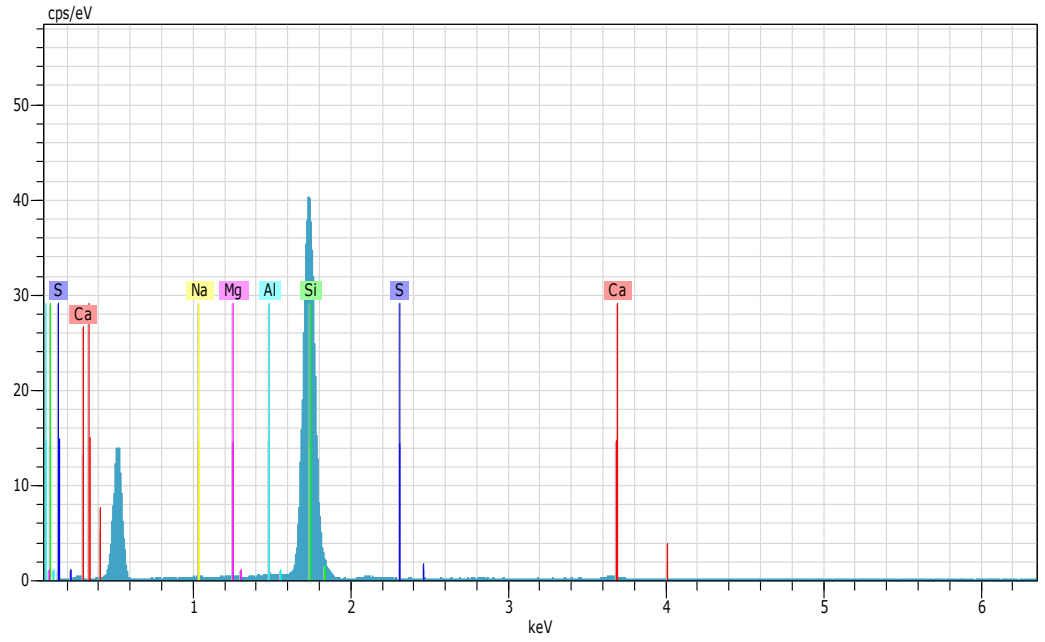

Fig. 4. A1 control specimen cured in magnesium sulphate solution with bladed-radial acicular thaumasite crystals and CSH-gypsum-calcite aggregates in matrix (SEM) (a) and elemental contents by EDAX (b)

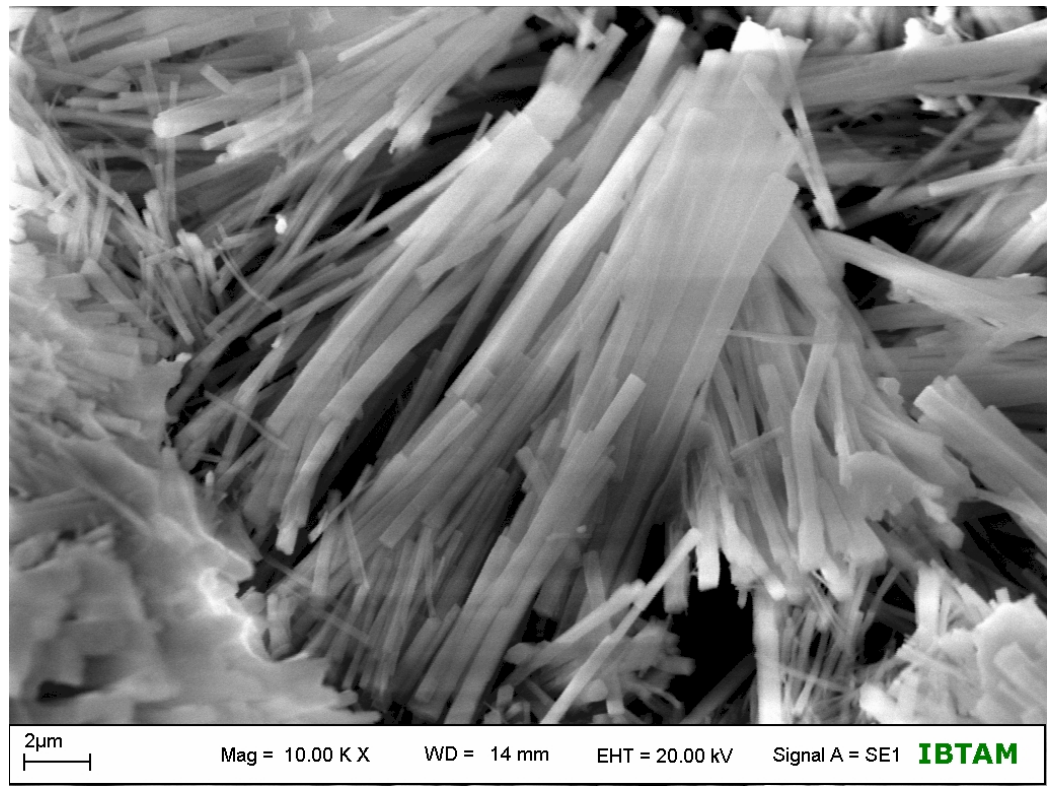

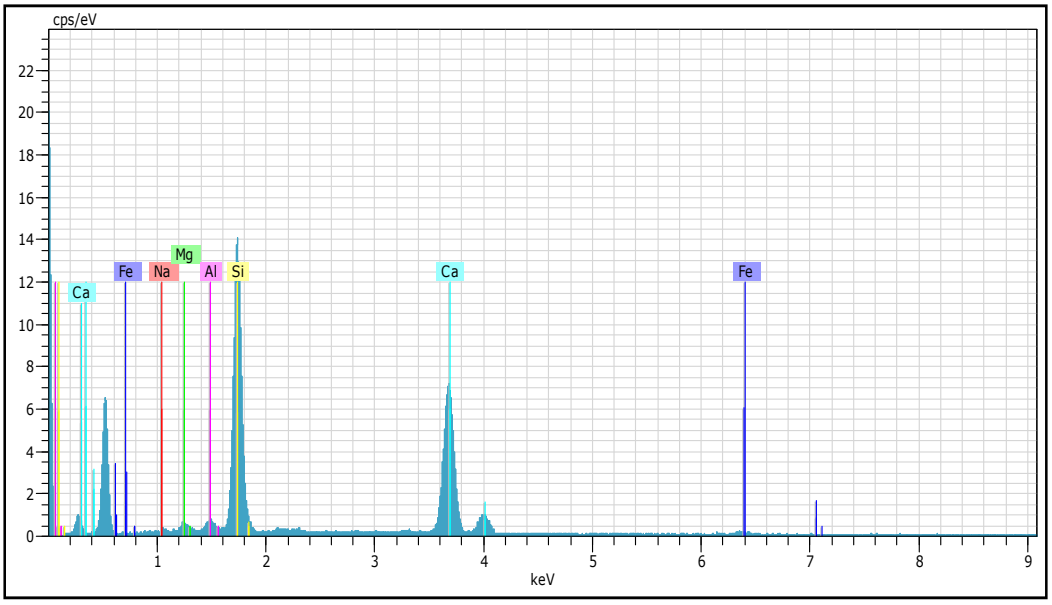

Fig. 5. A2 control specimen cured in magnesium sulphate solution with tabular minerals (SEM) (a) and elemental contents by EDAX (b)

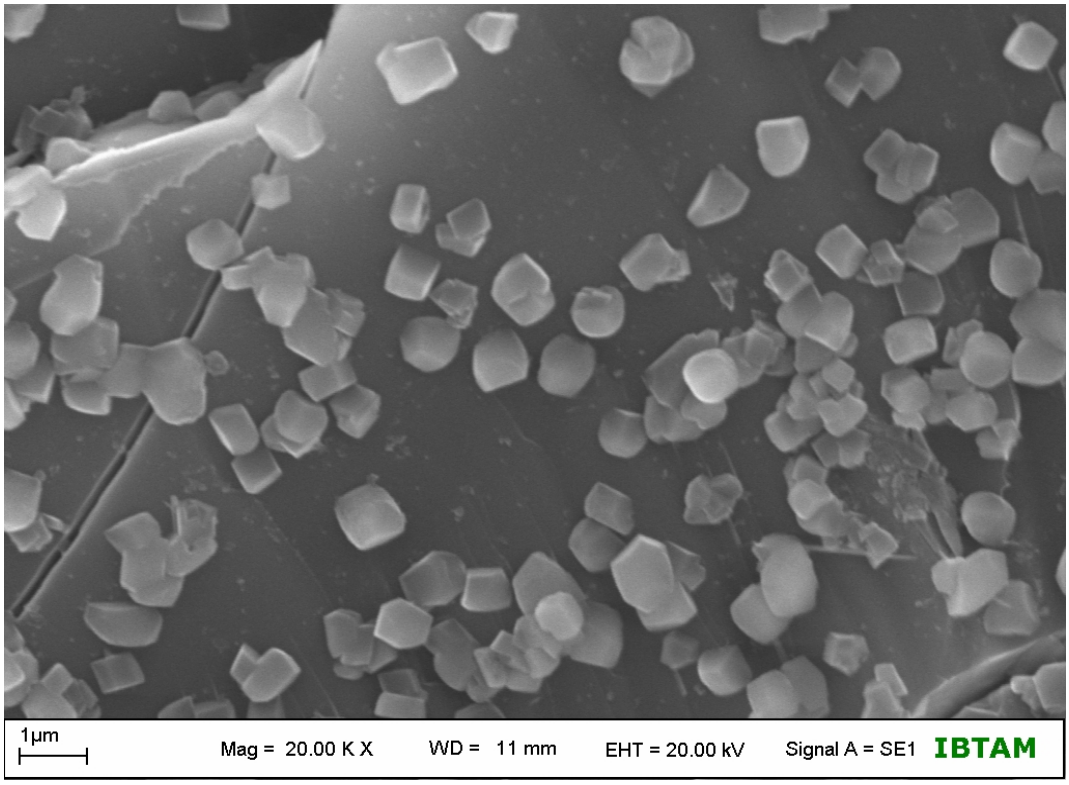

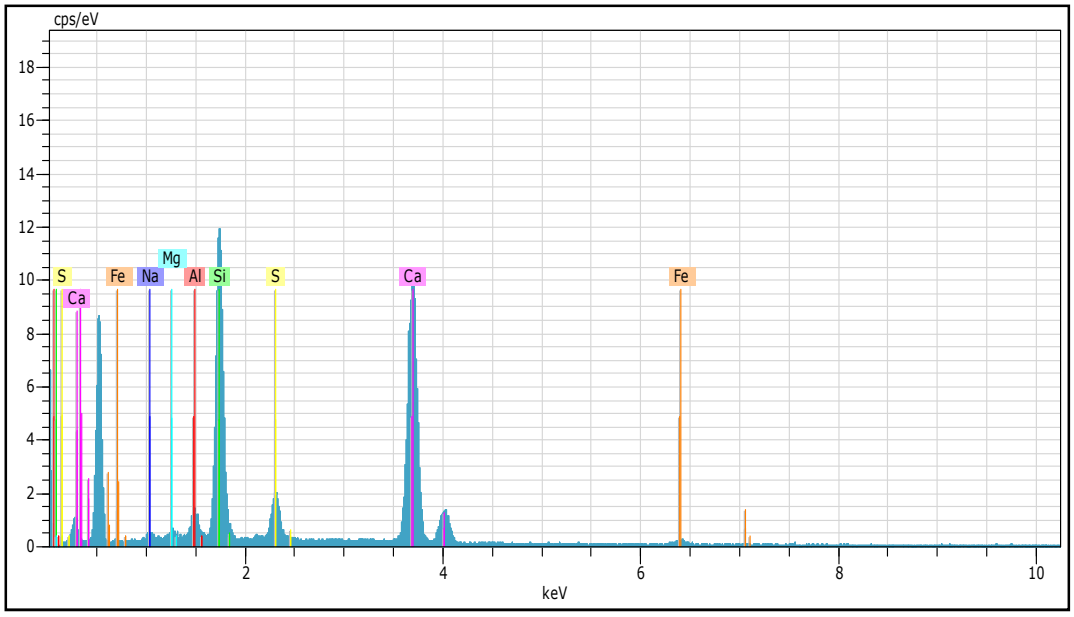

Fig. 6. Specimen B cured in magnesium sulphate solution with very fine 'pop corn' calcite and gypsum formed on quartz surface (SEM) (a) and elemental contents by EDAX (b)

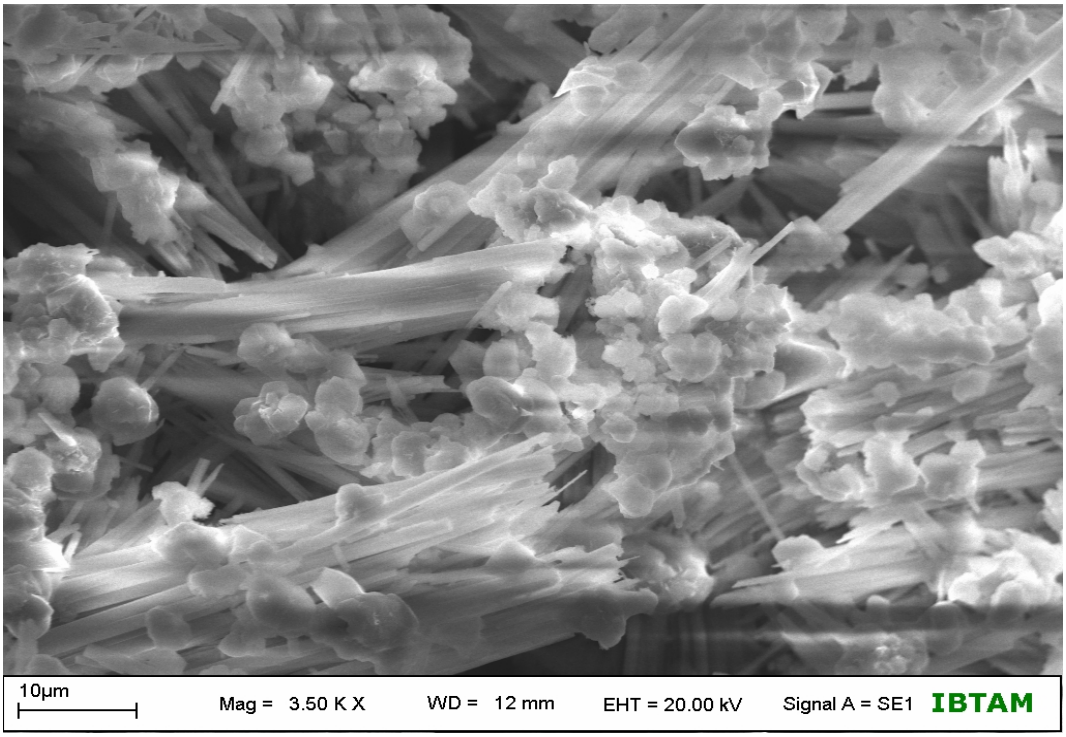

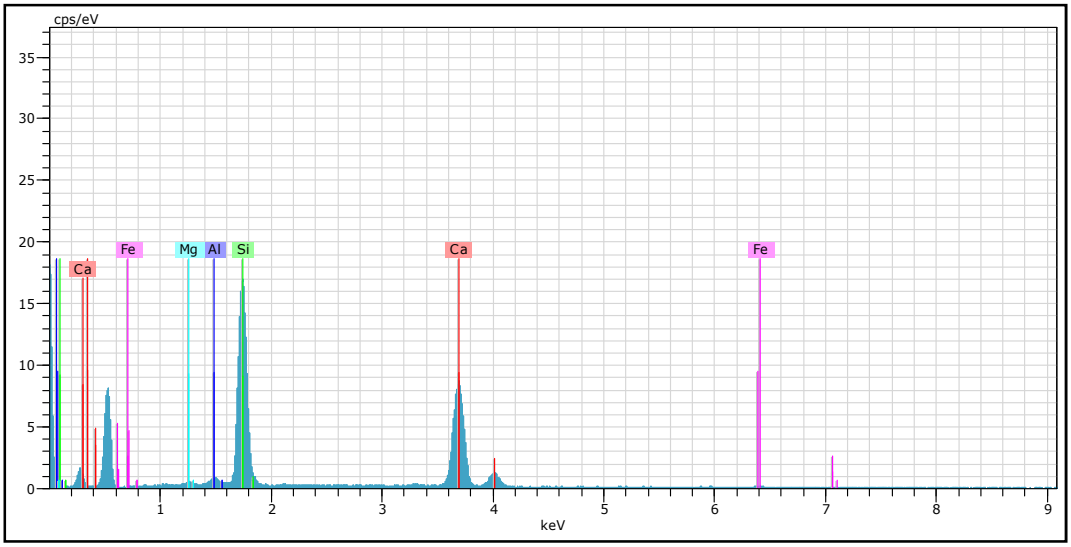

Fig. 7. Specimen C cured in magnesium sulphate solution. Bundles of randomly oriented thaumasite/ettringite fibers are closely packed/interlocked with clusters/aggregates of calcite and CSH structures (SEM) (a) and elemental contents by EDAX (b)

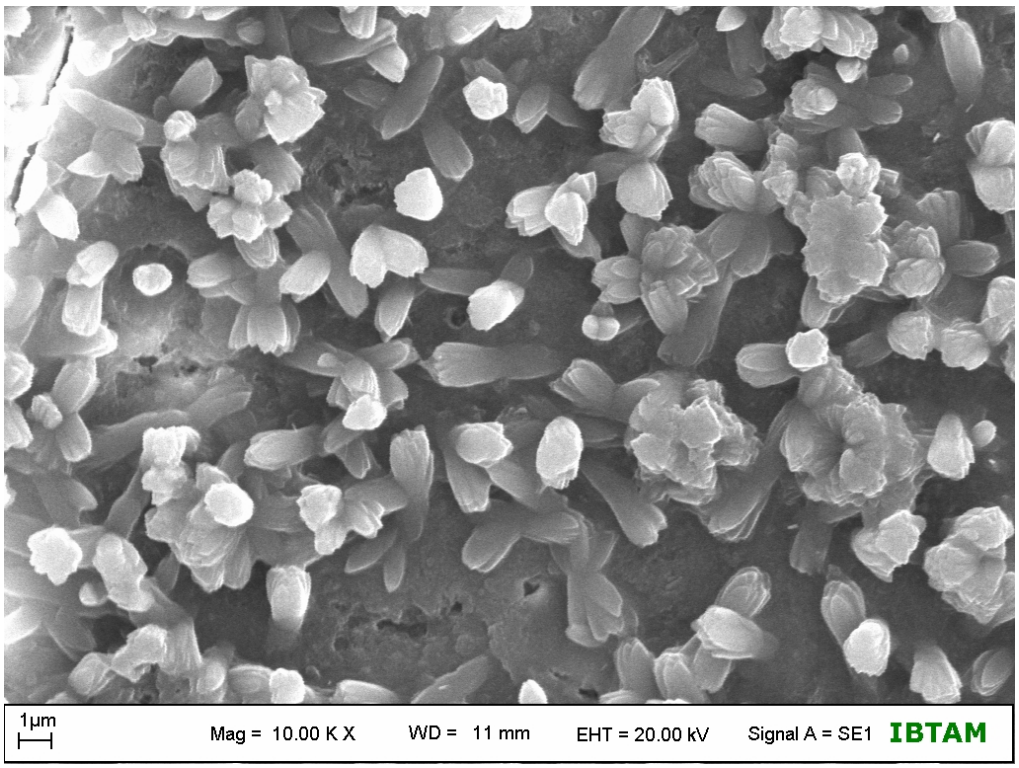

Fig. 8. Individual closely packed/interlocked coarser aggregates of calcite with gypsum, C-S-H structures and bundles of thaumasite and/or ettringite fibers (specimen C)

3.3.2 Polarised microscopy

The thin sections of the selected specimens cured in MgSO4 at room temperature conditions have revealed the presence of the CSH structures and the particular orientations of co-existing thaumasite and ettringite in the concrete blends. Yellowish domains of CSH structures, high first order bright yellow and low second order red to gray/blue thaumasite and grayish ettringite is frequent throughout the matrix of specimen A2 (Fig 11). Specimen A2 also reveals the presence of the tabular grains of thaumasite and ettringite that are also lining/forming along quartz grains and sinuous cracks [30] (Fig. 12). The flyash spherules of specimen B are also surrounded by in-situ forming thaumasite, ettringite and popcorn calcite as haloes most likely decreasing the strength of the mix as stated by Sibbick et al. [24,30] (Fig. 13).

3.3.3 Mineralogy

There is an increase in ettringite ($3CaO.Al_2O_3.3CaSO_4.31H_20$)/thaumasite ($CaSiO_3.CaCO3.CaSO_4.15H_2O$) (9.8, 5.6 Angstrom-contemporaneous peaks), ettringite (5.2, 4.7, 3.6, Angstrom), calcite/ettringite (3.8, 3.0 Angstrom-overlapping peaks) and thaumasite (3.5, 3.4 Angstrom) in specimen B (Fig. 14) and especially more prominently in specimen E (Fig. 15) compared to the lower contents in other specimens. The presence of higher amounts of silica and calcium compared to lower contents of alumina (Tables 5, 6 and Figs.

6, 7, 9 and 11) confirm the formation of thaumasite together with ettringite. Gypsum ($CaSO_4.2H_20$) (7.6 Angstrom) is also simultaneously transformed to ettringite and thaumasite during this process as a sequence of sulphate phase transformation especially in specimen E. The presence of portlandite ($Ca(OH)_2$) (4.9 Angstrom) in some specimens, as a mineral forming during the concrete curing process at low temperatures, may contain evidence of incomplete calcination during the concrete production or incomplete hydration on-going before and/or during the curing process.

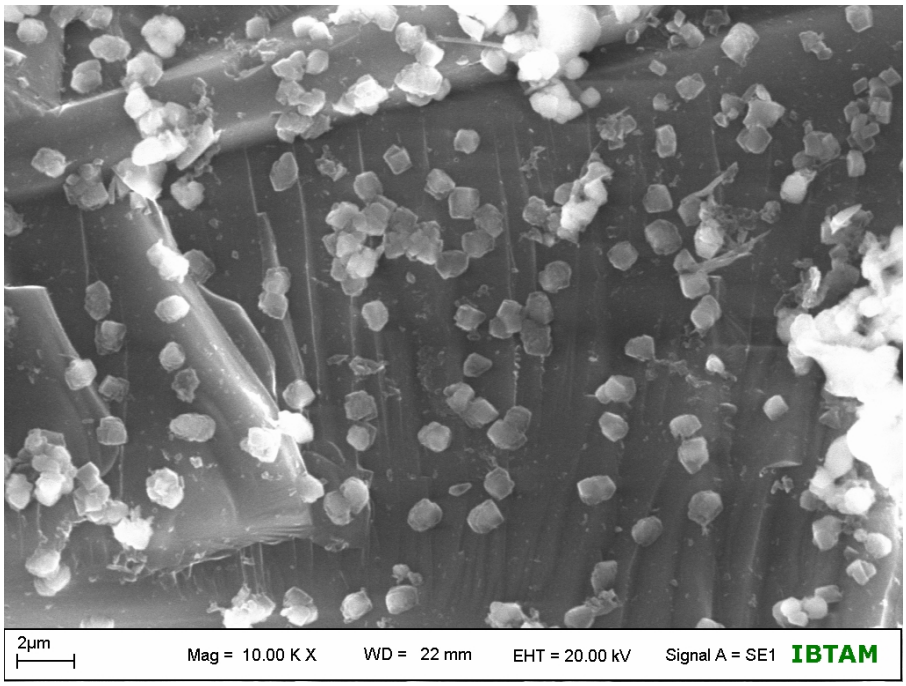

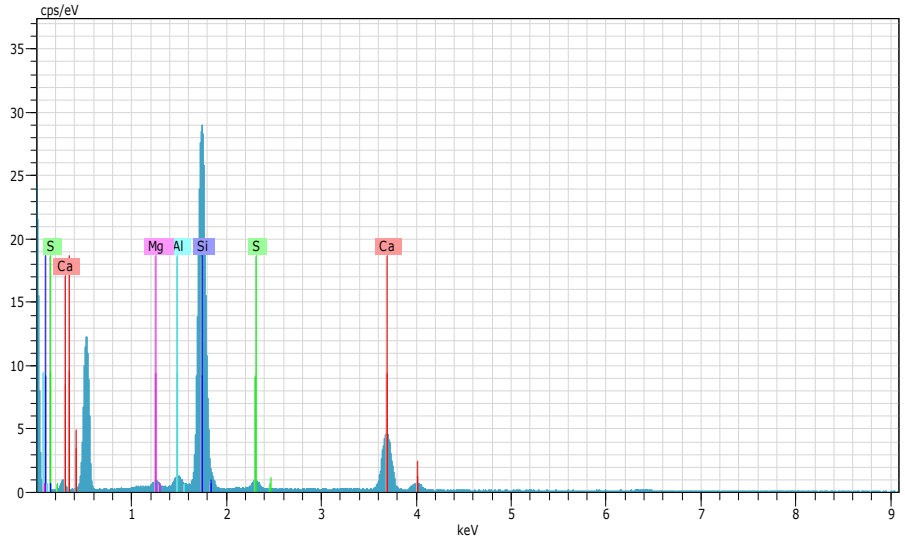

Fig. 9. Specimen D cured in magnesium sulphate solution. Popcorn Calcite on fractured mineral surface (a) and elemental contents by EDAX (b)

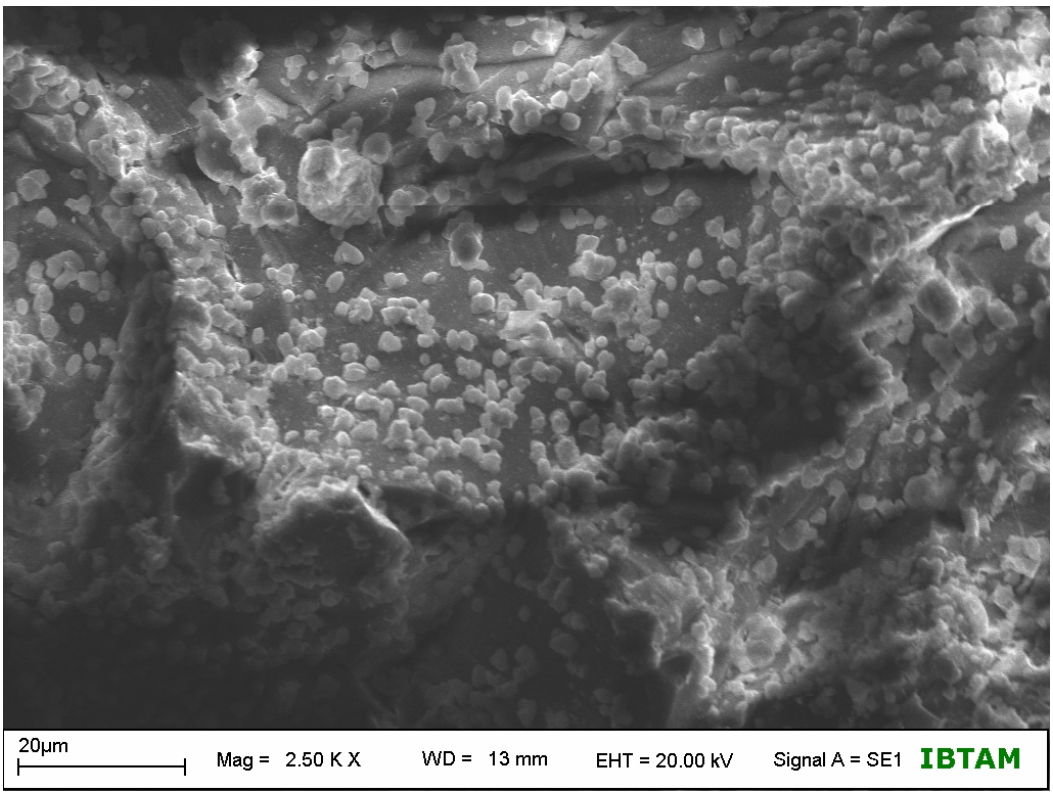

Fig. 10. Specimen E cured in magnesium sulphate solution. Grains of popcorn calcite with aggregates and domains of calcite, gypsum and structures alighning or randomly oriented on fractured and smooth/vitrified-like surfaces (a and b)

Theco-existing peaks of ettringite (9.8 A) and thaumasite (5.6 A) after the 10-year curing indicates an on-going and incomplete process of concretisation, which is ultimately anticipated to reach an ettringite-free thaumasite content. The detection of some of the weak and occasionally overlapping peaks of vaterite (popcorncalcite- polymorph of calcite-CaCO3) (3.55, 2.71, 2.10 Angstrom) which readily alter to calcite may also be the indicators of the beginning of the last-stage reaction as the pH of the cement pore fluids drops from 13 to neutral [30].

All these manifest the on-going transformation of the CSH gels and Ca $(OH)_2$ (portlandite) to ettringite and ultimately to thaumasite. Anorthite ($CaAl_2Si_2O_8$) (4.09 and 3.28 Angstrom) in specimen E is most likely a secondary formation rather than a flyash ingredient. The absence of quartz may be due to it's dissolution in specimen E during the uncontrollable pH process fluctuating between 8 to 13. This may have occurred during the curing process of specimen E that favoured the formation of the calcium and silica rich anorthite and subsequent formation of thaumasite. The vitrified-like surfaces observed by the SEM images of specimen E are most likely part of the quartz grains that resisted dissolution.

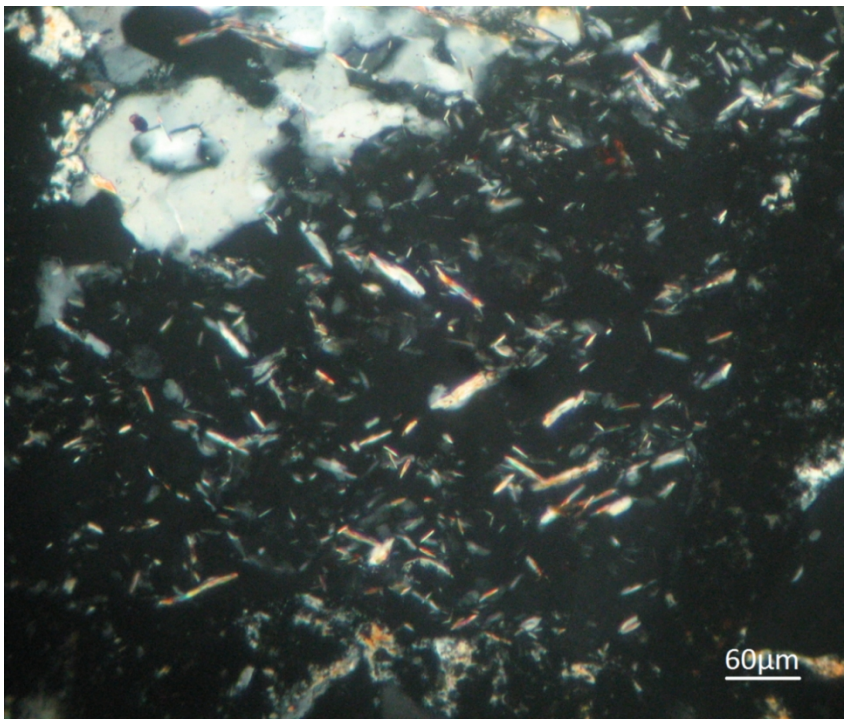

Fig. 11. Yellowish domains of CSH structures, tabular thaumasite (yellowish- red to grayish-blue) and ettringite (grayish) grains in matrix

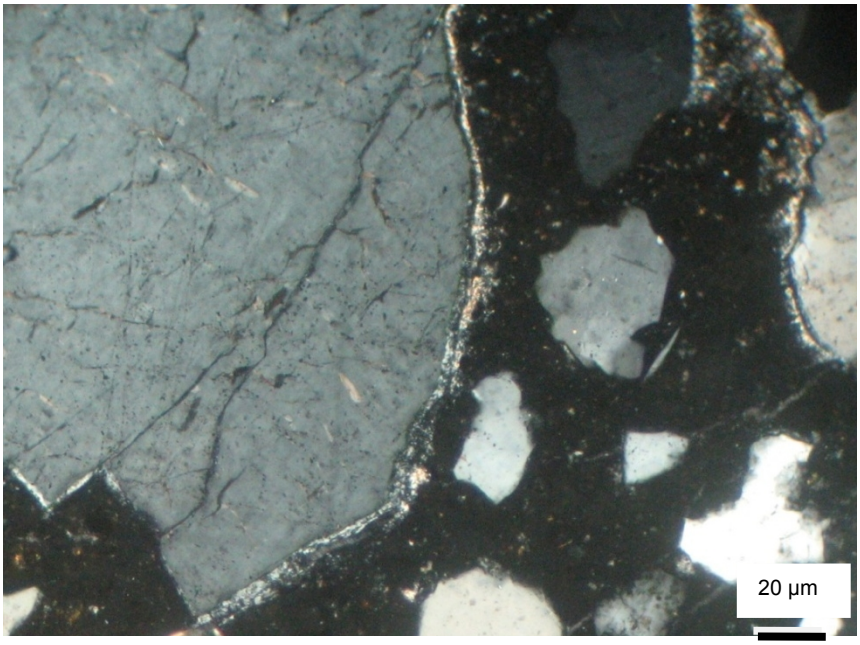

Fig. 12. Domains of thaumasite and ettringite surrounding larger grains and forming along mineral cracks of quartz

Table 5. Major chemical components of samples after detereoration

Sample	Element	Wt %	Atm %	Error
A1	Na	0.40	0.50	0.0
	Mg	0.26	0.31	0.0
	Al	1.13	1.18	0.1
	Si	94.57	95.21	1.7
	S	1.36	1.20	0.1
	Ca	2.28	1.61	0.1
A2	Mg	1.26	1.60	0.1
	Al	2.26	2.59	0.1
	Si	63.53	69.86	1.2
	S	2.86	2.76	0.1
	Ca	30.09	23.19	0.4
B	Na	0.92	1.41	0.1
	Mg	0.97	1.41	0.1
	Al	2.33	3.05	0.1
	Si	26.06	32.86	0.6
	S	2.28	2.52	0.1
	Ca	64.03	56.58	1.0
	Fe	3.42	2.17	0.1
C	Na	0.58	0.84	0.1
	Mg	1.41	1.94	0.1
	Al	1.90	2.35	0.1
	Si	42.75	50.94	1.0
	Ca	50.67	42.31	0.8
	Fe	2.69	1.61	0.1
D	Na	1.50	2.26	0.1
	Mg	1.03	1.46	0.1
	Al	2.99	3.83	0.1
	Si	27.77	34.18	0.7
	S	6.84	7.37	0.2
	Ca	56.76	48.97	1.0
	Fe	3.11	1.93	0.1
E	Mg	0.39	0.56	0.0
	Al	1.15	1.46	0.1
	Si	38.38	46.97	0.9
	Ca	57.91	49.67	0.9
	Fe	2.18	1.34	0.1

Table 6. Total elemental contents of specimen E (XRF)

Components	(%)	Error (%)
SiO_2	48.0780	0.1
CaO	28.1820	0.05
Al_2O_3	4.2417	0.02
SO_3	3.2994	0.02
Fe_2O_3	3.0571	0.02
MgO	1.5575	0.008
TiO_2	0.3683	0.007

Table 6 continued.....

Cl	0.3141	0.006
MnO	0.2031	0.004
Cr_2O_3	0.1664	0.004
K_2O	0.1495	0.002
P_2O_5	0,0945	0.002
Na_2O	0.0863	0.003
SrO	0.0559	0.001
NiO	0.0165	0.001
ZrO_2	0.0126	0.001
ZnO	0.0098	0.001
CuO	0.0074	0.001
L.I	10.1	0.0001

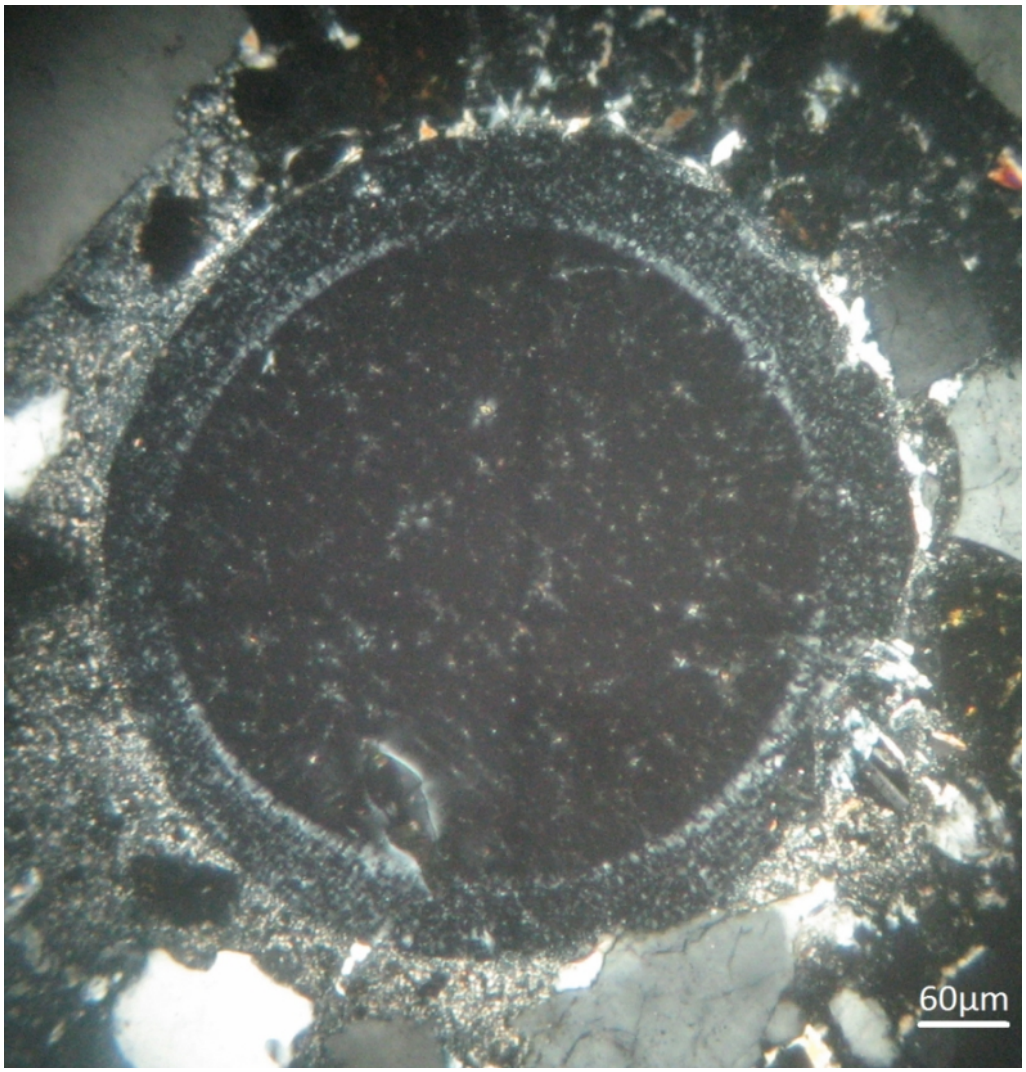

Fig. 13. Thaumasite, ettringite and popcorn calcite surrounding fly ash spherules

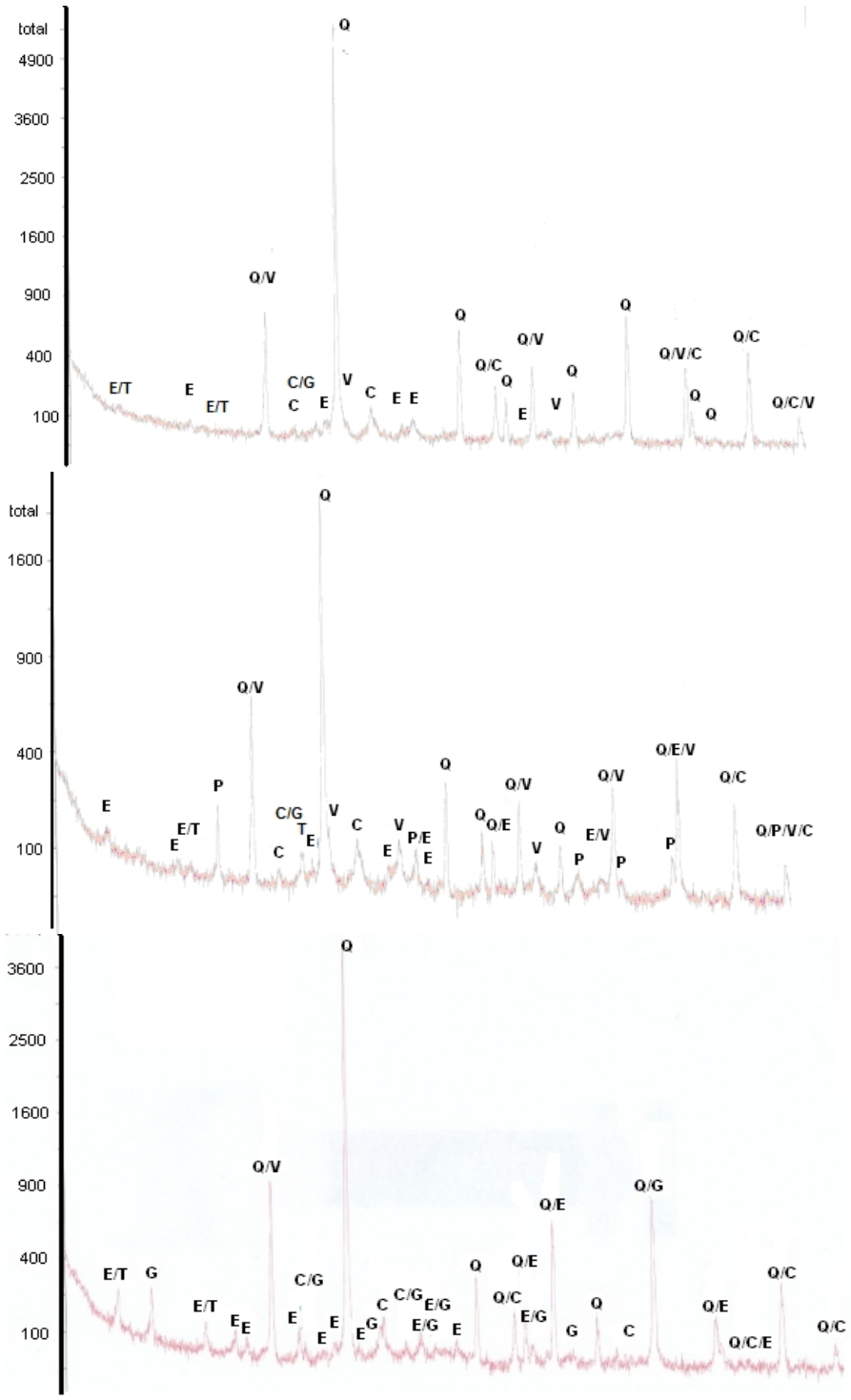

Fig. 14. X-ray diffractograms of the cured specimens (Specimens A1, A2, and B)
(A: Anorthite; C: Calcite; E: Ettringite; G: Gypsum; P: Portlandite; T: Thaumasite; Q: Quartz; V: Vaterite)

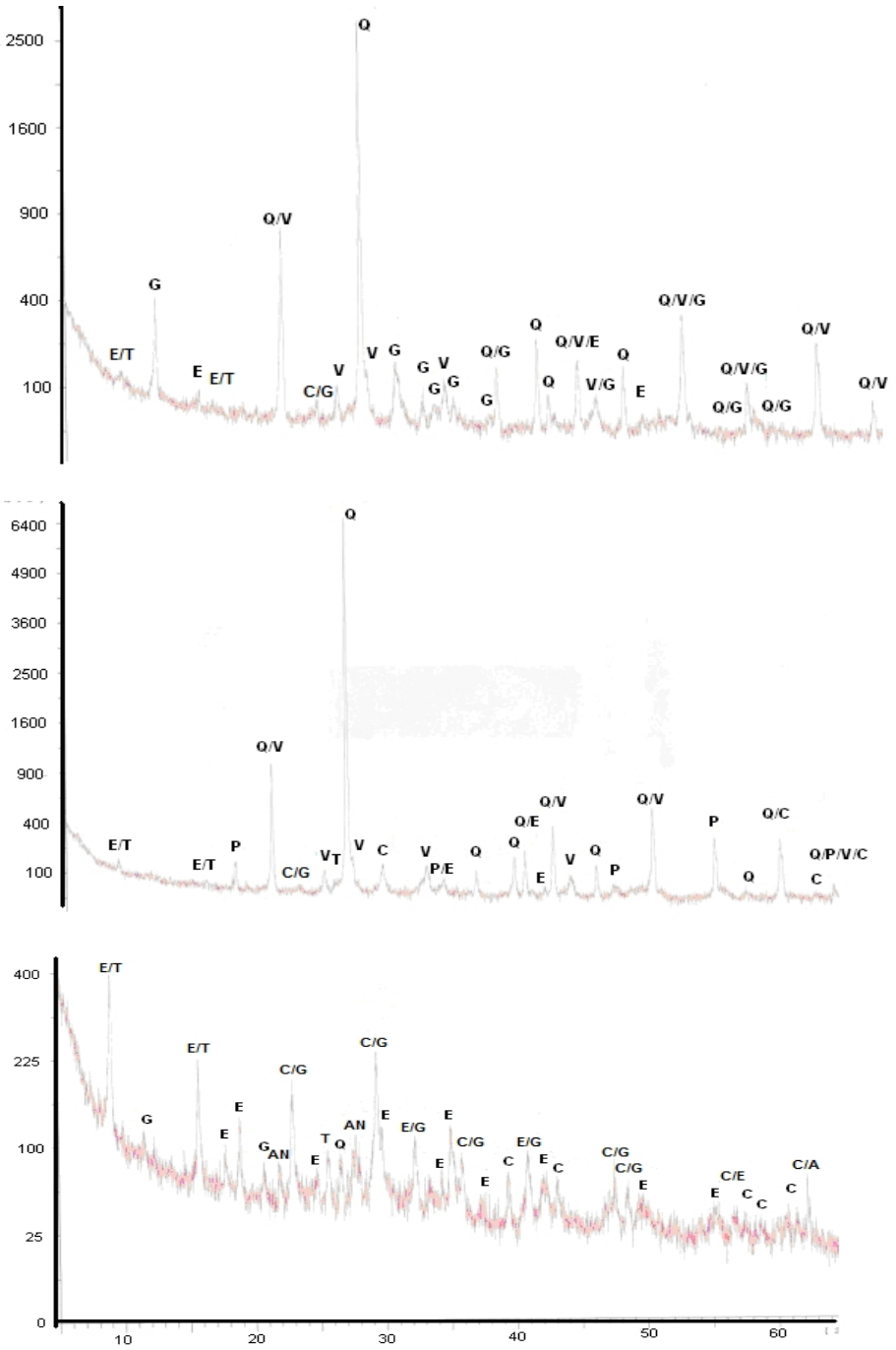

Fig. 15. X-ray diffractograms of the cured specimens (Specimens C, D, and E)
(A: Anorthite; C: Calcite; E: Ettringite; G: Gypsum; P: Portlandite; T: Thaumasite; Q: Quartz; V: Vaterite)

4. CONCLUSION

The study revealed that the,

1. The higher pressure resistance of the C and E specimens compared to the B and D was most likely due to higher CSH gel/aggregate formation together with the co-existing interlocked thaumasite and ettringite crystals.
2. The interground specimen resistance was higher than the separate ground blends, most likely due to the fineness of the material. But the lower resistance of D than E was most probably due to the abundant popcorn calcite distribution and the cracks developed in the former.
3. The use of the ground granulated blast furnace slag and basaltic pumice improved the sulphate resistance of the cement mortars, where specimen E yielded the highest sulphate resistance-highest TSA resistance.
4. The microstructure was modified with the addition of pozzolans. The effect of this was a reduced rate of leaching of the alkali hydroxide from the pore fluid but did not prevent expansion.
5. Despite the numerous studies conducted on the relation of hydration and hydrolysis with reference to cement hardening, the hydration-bound hardening phenomenon coupled with thaumasite morphology and matrix and/or pore space orientations are in need of further investigation. Nevertheless, the presence of thaumasite together with ettringite and portlandite in some specimens reflect the incomplete transformation phase to hydration, i.e., the anticipated complete transformation of ettringite to thaumasite [18- 23] and may indicate the continuity of the TSA process in concrete.

ACKNOWLEDGEMENTS

The authors acknowledge the valuable laboratory assistance for the XRD and SEM analyses given by the Iskenderun Cement Manufacturers Association throughout the study period and also to Profs. ErdoganBada (Çukurova University) and Mike Hayden (Springer publishers language editorial) for their invaluable efforts in refining the language.

COMPETING INTERESTS

Authors have declared that no competing interests exist.

REFERENCES

1. Higgins DD. Ground granulated blast furnace slag. World Cem. 1995;6:51–2.
2. Roy DM, Idorn GM. Hydration, structure and properties of blast furnace cements, mortar, concrete. ACI J. 1982;21:444–57.
3. Zhang YM, Napier TJ. Effects of particle size distributions, surface area and chemical composition on Portland cement strength. Powder Technol. 1995;83:245–52.
4. Binici H, Aksogan O, Kaplan H. A study on cement mortars incorporating plain Portland cement (PPC), ground granulated blast-furnace slag (GGBFS) and basaltic pumice. Indian Journal of Engineering & Materials Sciences. 2005;12:214-220.
5. Binici H, Arocena J, Kapur S, Aksogan O, Kaplan H. Microstructure of red brick dust and ground basaltic pumice blended cement mortars exposed to magnesium sulphate solutions. Canadian Civil Engineering Journal. 2009;36:1784-1793.

6. Binici H, Aksogan O. Sulphate resistance of plain and blended cement. Cement and Concrete Composite. 2006;28:39-46.
7. Park YS, Suh JK, Lee JH, Shin YS. Strength deterioration of high strength concrete in sulphate environment. Cem Concr Res. 1999;29:1397–402.
8. Verbeck GJ. In performance of concrete. Toronto: University of Toronto Press. 1968;35–41.
9. Irasar EF, Gonzalez M, Rahhal V. Sulphate resistance of type V cements with limestone filler and natural additive. Cem Concr Compos. 2000;22:361–8.
10. ACI Committee 201. Guide to durable concrete. ACI Mater J. 1991;88:54–82.
11. Turkmenoglu AG, Tankut A. Use of tuffs from central Turkey as admixture in pozzolanic cements. Cem Concr Res. 2002;22:629–37.
12. Yeginobalı A, Sobolev KG, Soboleva SV, Kıyıcı B. Termal Resisitance of Blast Furnace Slag High Strength Concrete Cement. 1st International Symposium on Mineral Admixtures in Cement, İstanbul; 1997.
13. Massazza F. Puzolana and Pozzolanic Cement. Arnold, London. 1998;574-581.
14. Crammond NJ. The thaumasite form of sulphate attack in the UK. Cement and Cement Composites. 2003;8:809-815.
15. Binici H, Kapur S, Arocena J, Kaplan H. The sulphate resistance of cements containing red brick dust and ground basaltic pumice with sub-microscopic evidence of intra-pore gypsum and ettringite as strengtheners. Cement and Concrete Composites. 2012;34:279–287.
16. TSEN 12142. Turkish Standards, Turkey; 1997. [in Turkish].
17. European Standard ENV 197-1. Cement-composition. Specifications and Conformity Criteria; 1995.
18. Al-Amoudi OSB. Performance of 15 reinforced concrete mixtures in magnesium-sodium sulphate environments. Constr Build Mater. 1995;9:149-158.
19. Page CL, Page MM. Durability of concrete and cement composites, Cambridge England: CRC Press; 2007.
20. Sibbick RG, Crammond NJ, Metcalf D. The microscopic characterisation of thaumasite. Cement and Cement Composites. 2003;8:831-837.
21. Brown PW, Hooton RU, Clark DA. The co-existence of thaumasite and ettringite in concrete exposed to magnesium sulphate at room temperature and the influence of blast furnace slag substitution on sulphate-resistance. Cement and Concrete Composites. 2003;25939-945.
22. Ramlochan T, Thomas MDA, Hooton RD. The effect of pozzolans and slag on the expansion of mortars cured at elevated temperature Part II: Microstructural and microchemical investigations. Cement and Concrete Research. 2004;34:1341–1356.
23. Macphee D, Diamond S. Thaumasite in cementitious materials. Cement and Concrete Composites. 2003;25(8):1045–1050.
24. Sibbick T, Fenn D, Crammond NJ. The occurrence of thaumasite as a product of seawater attack. Cement and Concrete Composites. 2003;25-8:1059-1066.
25. Shi C, Wang D, Behnood A. Review of thaumasite sulphate attack on cement mortar and concrete. Journal of Materials in Civil Engineering. 2012;24:1450-1460.
26. Brown PW, Hooton RD, Clark BA. Microstructural changes in concretes with sulfate exposure. Cement and Concrete Composites. 2004;26:993-999.
27. Ramezanianpour A, Hooton R. Sulfate resistance of Portland-limestone cements in combination with supplementary cementitious materials. Materials and Structures. 2013;46:1061-1073.
28. Mittermayr F, Baldermann A, Kurta C, Rinder T, Klammer D, Leis A, Tritthart J, Dietzel M. Evaporation a key mechanism for the thaumasite form of sulfateattack. Cementand Concrete Research. 2013;49:55–64.

29. Komljenovic M, Baščarević Z, Marjanović N, Nikolić V. External sulfate attack on alkali-activated slag. Construction and Building Materials. 2013;49:31-39.
30. Sibbick T, Crammond N. Microscopical investigations into recent field examples of the thaumasite form of sulfate attack (TSA). In: Proc. of the 8th Euroseminar on Microscopy Appliedto Building Materials. Athens, Greece. 2001;261–269.
31. Kelling G, Kapur S, Sakarya N, Akca E, Karaman C, Sakarya B, Robinson P. Basaltic Tephra: Potential new resource for ceramic industry. British Ceramic Transactions. 2000;99:129–136.
32. Fitzpatrick EA. Soil microscopy and micromorphology. John Wiley & Sons Ltd. Chichester, England. 1993;304. ISBN 0-471-93859-9,
33. CEN/TR 15697. Cement – performance testing for sulfate resistance. State of the Art Report; 2008.

Peer-review history:
The peer review history for this paper can be accessed here:
http://www.sciencedomain.org/review-history.php?iid=635&id=5&aid=5914